analytical chemistry

Technical Note

pubs.acs.org/ac

Continuous-Ink, Multiplexed Pen-Plotter Approach for Low-Cost, High-Throughput Fabrication of Paper-Based Microfluidics

Reza Amin,[†,×] Fariba Ghaderinezhad,[†,×] Lu Li,[†,‡] Eric Lepowsky,[†] Bekir Yenilmez,[†] Stephanie Knowlton,[§] and Savas Tasoglu*[,†,‡,§,∥,⊥]

[†]Department of Mechanical Engineering, University of Connecticut, Storrs, Connecticut 06269, United States

[‡]The Connecticut Institute for the Brain and Cognitive Sciences, University of Connecticut, 337 Mansfield Road, Storrs, Connecticut 06269, United States

[§]Department of Biomedical Engineering, University of Connecticut, Storrs, Connecticut 06269, United States

[∥]Institute of Materials Science (IMS), University of Connecticut, 97 North Eagleville Road, Storrs, Connecticut 06269, United States

[⊥]Institute for Collaboration on Health, Intervention, and Policy (InCHIP), University of Connecticut, 2006 Hillside Road, Storrs, Connecticut 06269, United States

Supporting Information

ABSTRACT: There is an unmet need for high-throughput fabrication techniques for paper-based microanalytical devices, especially in limited resource areas. Fabrication of these devices requires precise and repeatable deposition of hydrophobic materials in a defined pattern to delineate the hydrophilic reaction zones. In this study, we demonstrated a cost- and time-effective method for high-throughput, easily accessible fabrication of paper-based microfluidics using a desktop pen plotter integrated with a custom-designed multipen holder. This approach enabled simultaneous printing with multiple printing heads and, thus, multiplexed fabrication. Moreover, we proposed an ink supply system connected to commercial technical pens to allow continuous flow of the ink, thereby increasing the printing capacity of the system. We tested the use of either hot- or cold-laminating layers to improve (i) the durability, stability, and mechanical strength of the paper-based devices and (ii) the seal on the back face of the chromatography paper to prevent wetting of the sample beyond the hydrophilic testing region. To demonstrate a potential application of the paper-based microfluidic devices fabricated by the proposed method, colorimetric urine assays were implemented and tested: nitrite, urobilinogen, protein, blood, and pH.

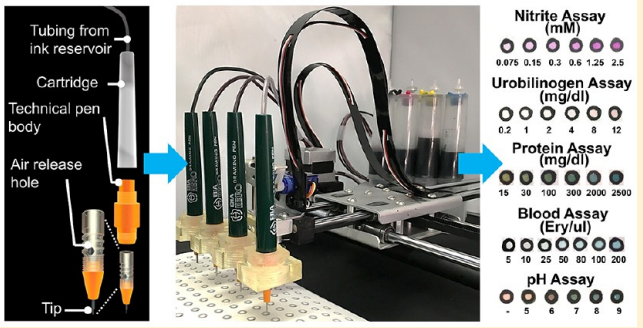

Microanalytical devices enable point-of-care diagnostics in a multitude of fields,[1−6] including, but not limited to, the medical field,[7,8] environmental and food safety,[9−13] chemistry,[14] and forensics.[15] Microfluidic devices can greatly benefit from low-cost, readily available materials as well as simple and rapid fabrication processes. Specifically, paper-based microfluidic devices offer a low-cost, high-throughput, and disposable alternative[16−19] due to their affordability and ease of manufacturing.[18] Several approaches to high-throughput fabrication of paper-based microfluidic devices have been recently presented.[20−24]

According to the World Health Organization (WHO), the most effective way to increase access to medical diagnostics in developing countries is to provide these communities with tools for accessible and affordable local production.[25] In response to this need, we have developed an approach using a desktop pen plotter integrated with a custom-designed multipen holder for low-cost and multiplex prototyping of paper-based microfluidics. Permanent markers were used to form a hydrophobic barrier delineating the hydrophilic zones through which the liquid sample travels due to capillary action. The markers were chosen as the patterning agent due to their hydrophobicity and the use of a colorant for visualization of the printed pattern.[26] A custom-designed multipen holder was 3D-printed and enabled multiplex plotting (Figure 1a,b). We also implemented a continuous ink system to continuously supply ink to the technical pens and thereby further improve the cost-effectiveness and throughput of fabrication compared to relying on fixed-volume permanent markers (Figure 1c,d). We incorporated a laminating layer to the fabricated paper-based microfluidic devices to (i) improve their durability, stability, and mechanical strength; (ii) ensure the stability of the hydrophobic barriers and biochemical reagents during storage.[27] To demonstrate the diagnostic applications of resulting paper-based assays, we conducted colorimetric tests for five

Received: April 16, 2017
Accepted: May 30, 2017
Published: June 9, 2017

DOI: 10.1021/acs.analchem.7b01418
Anal. Chem. 2017, 89, 6351−6357

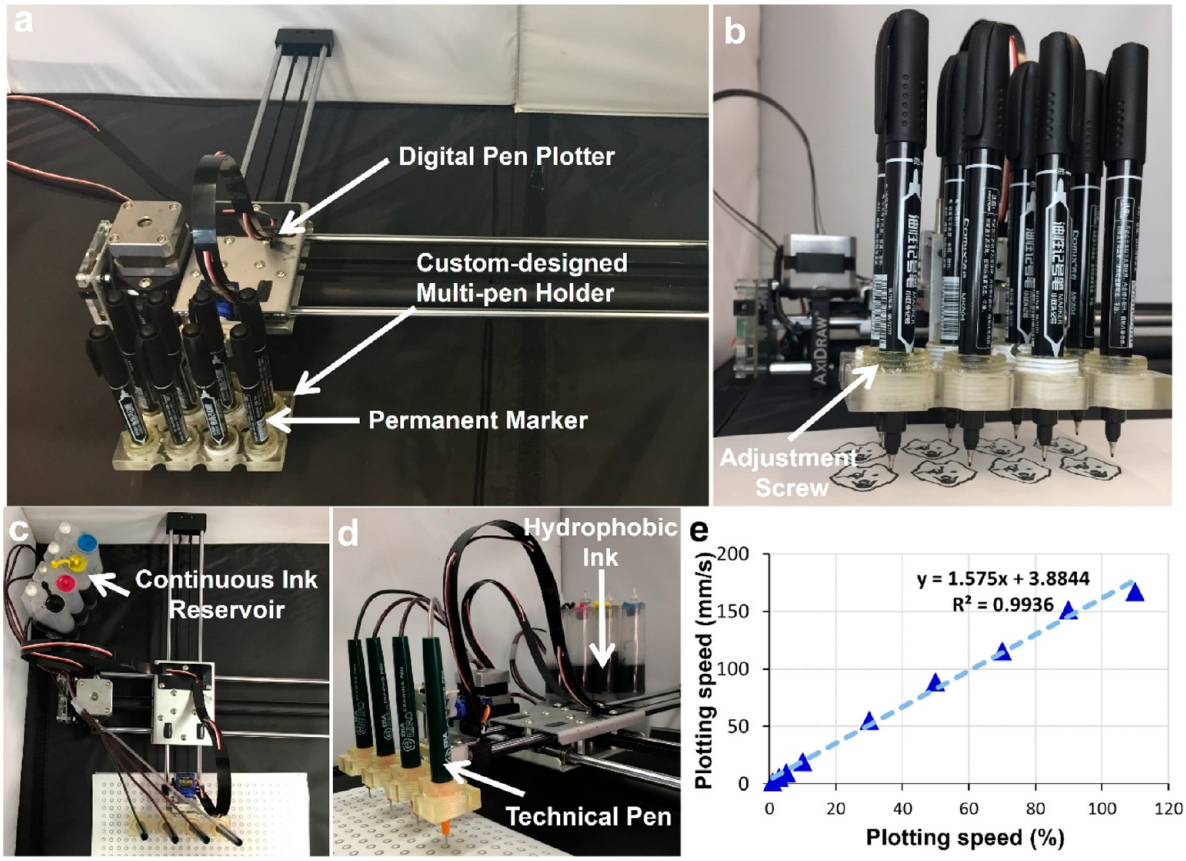

Figure 1. Multipen plotter for fabricating paper-based microfluidics. (a) Desktop pen plotter integrated with custom-designed multipen holder. (b) Low-cost, 3D-printed multipen holder, which was custom-designed to increase the throughput of the setup. (c) Top-view and (d) side-view of the continuous ink system (ink reservoir) integrated with the pen plotter with multipen holder. (e) Plotting speed in units of mm/s vs percentage; linear velocity (mm/s) was calculated by measuring the time needed for plotting a 25 cm line with a fine-tip Comix marker.

analytes found in urine: nitrite, urobilinogen, protein, blood and pH.

RESULTS AND DISCUSSION

Design and 3D Printing of a Multipen Holder. To increase the throughput of the fabrication, a multipen holder was designed to align eight markers such that they would be attached to the plotter and plot the pattern in parallel (Figure 2a). The height of each marker can be separately and precisely adjusted using threaded fittings on the pen holder to make the pressure of each pen on the paper consistent and decrease the deflection of the pen against the paper (Figure 1b). As the speed of the plotter can be adjusted based on the percentage of the maximum linear speed, we converted the nondimensional unit (%) to linear speed (mm/s) (Figure 1e); therefore, 30% speed is equivalent to 55.3 mm/s.

To characterize the accuracy of the plotting at 30% plotting speed, a 12 × 12 pattern of circles was plotted by both the fine- and broad-tip Comix markers (Figure 2b). The trueness and the precision of this process were measured. X and Y are defined for each marker as the error in the plotting (i.e., the deviation of the center of the plotted circle from the position defined in the design) in the X- and Y-directions, respectively. $\overline{X}$ and $\overline{Y}$ are the averages of X and Y over the set of eight markers, including 12 trials. Therefore, $\overline{X}$ and $\overline{Y}$ represent the truenesss of the plotting approach. These values are 0.40 mm and 0.55 mm for the fine tip, respectively, and 0.40 mm and 0.54 mm for the broad tip, respectively.

The error in the X- and Y-directions can therefore be defined as $X-\overline{X}$ and $Y-\overline{Y}$. The results of 12 circles plotted with eight different markers were plotted, and a 95% confidence ellipse was plotted using the 2σ values in the X- and Y-directions to quantify the precision (Figure 2c,e). The ellipse for the fine tip (0.80 mm by 1.22 mm in the X- and Y-directions, respectively) was larger than that of the broad tip (0.45 mm by 1.11 mm in the X- and Y-directions, respectively), indicating that a greater precision can be attained with the broad tip. The results show that the pens which are farther from the support (pens 1, 4, 5 and 8) have a larger deflection in both the X- and Y-directions. This may be partially due to the lower stability of the holder in the corners, which allows more deflection when the markers meet the paper.

The deflections of the circles plotted using the fine-tip and broad-tip of the single marker vs the eight markers have been investigated. Our results show that the accuracy of the single-marker-drawing was higher than the accuracy of the eight marker drawing. The trueness of the single pen plotting approach was measured to be −0.02 mm and 0.14 mm for the fine tip, and 0.06 mm and −0.43 mm for the broad tip, in the X- and Y-directions, respectively. The 2σ values (95% confidence ellipse) in the X- and Y-directions were calculated to be 0.36 mm by 0.28 mm, respectively, for the fine tip and 0.39 mm by 0.27 mm, respectively, for the broad tip (Figure S-1 and Table S-1).

The effects of different plotting speeds on the accuracy were also quantified. Figure 2d,f displays the deflection of the

DOI: 10.1021/acs.analchem.7b01418
Anal. Chem. 2017, 89, 6351−6357

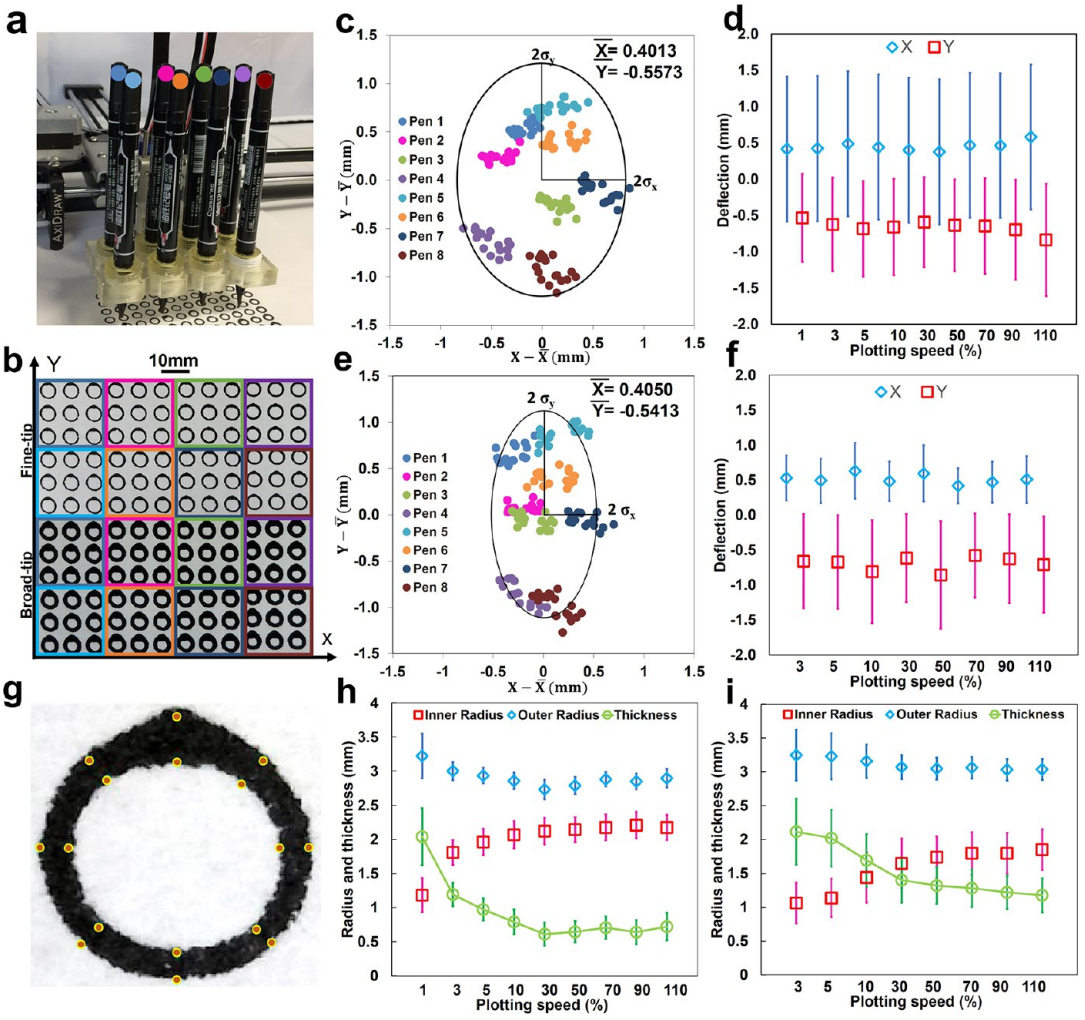

Figure 2. Accuracy of plotted patterns using the multipen holder with eight pens. (a) Custom-made, 3D-printed multipen holder integrated with the pen plotter. (b) Printed circle pattern with the both fine- and broad-tips of the Comix marker using the multipen holder. (c) Deflection of the plotted patterns with the fine tip of eight Comix markers in both the *X*- and *Y*-directions. (d) The mean and standard deviation (STD) of the deflection of the plotting system (all eight pens) when plotting with fine tip at different plotting speeds (n = 9). (e) Deflection of the plotted patterns with the broad tip of eight Comix markers in both the *X*- and *Y*-directions. (f) The mean and standard deviation (STD) of deflection of the plotting system (all eight pens) when plotting with the broad tip at different plotting speeds (n = 9). (g) Representative method of measuring the inner and outer radii of the plotted circles at eight different points (at angles of 0−315° with an interval of 45°) with MATLAB scripts. The mean and standard deviation of inner and outer radii of the plotted patterns at different plotting speeds with the (h) fine tip and (i) broad tip of the Comix marker. σ_x and σ_y are the total standard deviations in *X*- and *Y*-directions, respectively. $\bar{X}$ and $\bar{Y}$ are the mean deflections in the *X*- and *Y*-directions, respectively.

patterns plotted at different speeds with both the fine and broad tips. The results show that the deflection for both tips is in the same range; furthermore, the speed has little influence on the deflection, which means that the multipen holder could work well at different plotting speeds. The plotting speed does not significantly affect the trueness or precision of the plotting.

We also investigated the roundness of the plotted circles. The inner and outer radii of the circles were measured at 45° intervals using a MATLAB script, as shown in Figure 2g. Figure 2h,i shows the inner and outer radii of the plotted patterns as a function of plotting speed for the fine and broad tips. The standard deviation in the plotted radii is a measure of roundness; the roundness is better when using the fine tip. The roundness decreases significantly at lower plotting speeds and plateaus around 30% plotting speed. The line thickness is also shown as the difference between the inner and outer radii. Further, the plotting speed affects the time the marker spends in contact with the paper and, therefore, the amount of ink deposited. As expected, by increasing the plotting speed, the inner and outer radii of the circles decrease, resulting in a smaller line thickness; the thickness plateaus at speeds more than 30%.

Lamination of the Paper. Since the paper used here is made of cellulose, which loses its mechanical properties upon wetting, we applied a lamination layer on the back of the paper (opposite of the patterned side) to improve the durability, stability, and mechanical strength. Figure 3a shows an SEM image of a cross-section of the paper with a hot- and cold-lamination layer. We investigated the difference in plotting before and after laminating the papers and compared their performances at different plotting speeds using both fine and broad tips. We plotted circles with diameters of 4 mm and used a dyed aqueous solution to test the water resistance of the patterns. The results are presented in Figure 3b and are

DOI: 10.1021/acs.analchem.7b01418
Anal. Chem. 2017, 89, 6351−6357

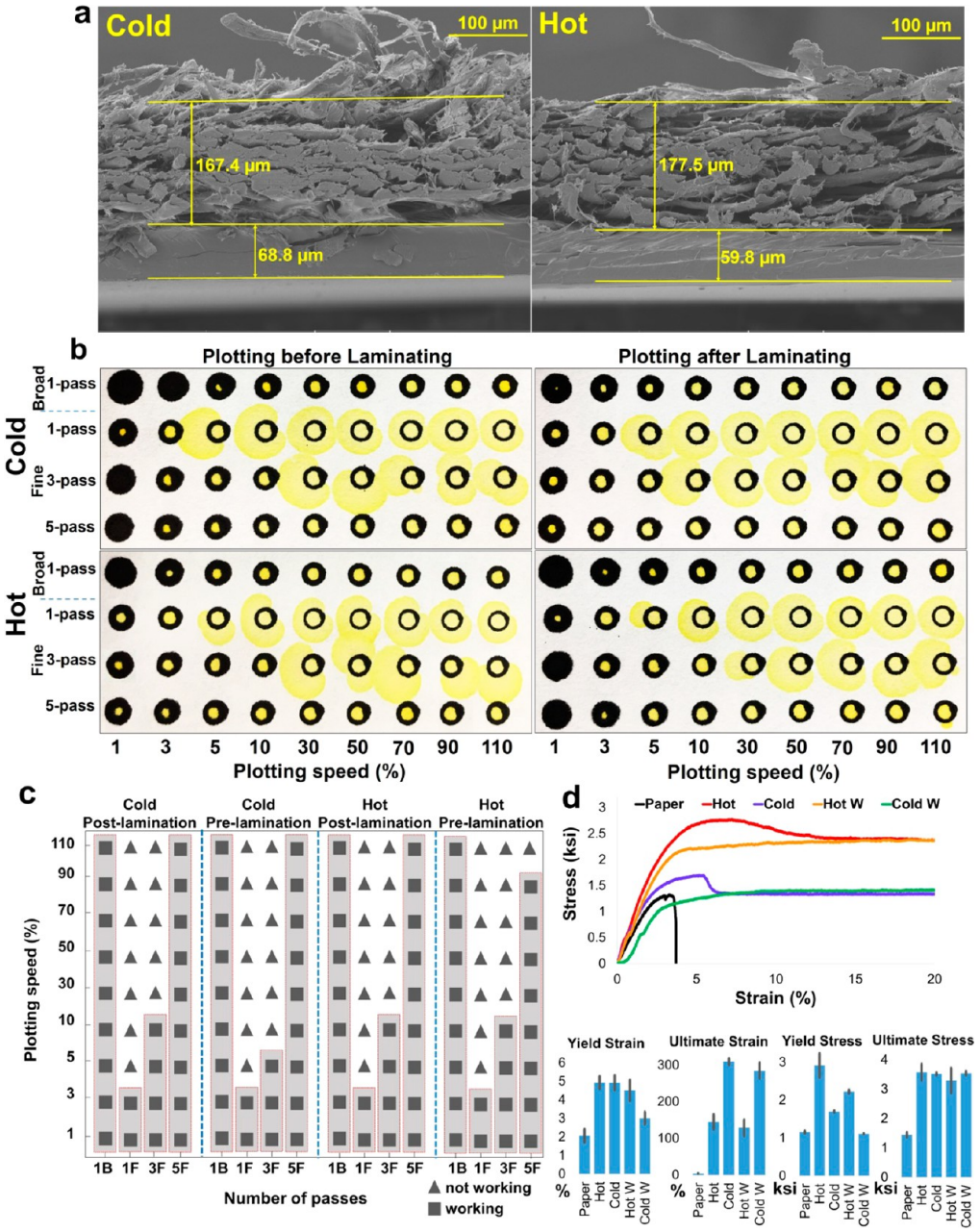

Figure 3. Characteristics of the laminating layer and its effect on the performance of the fabricated device. (a) SEM image of the cross section of hot- and cold-laminated papers. (b) Effect of different plotting speeds and number of passes on water resistance of patterns before and after laminating the paper. (c) The summarized results of (b) as a performance chart. 1B stands for 1-pass of broad tip and 1F, 3F, and 5F stands for 1-pass, 3-pass, and 5-pass of fine tip respectively. (d) Stress–strain curves of laminated papers. Hot W and Cold W stands for wetted hot laminated paper and wetted cold laminated paper.

summarized in Figure 3c. The results of the two studied cases (plotting before and after laminating) are very similar, which gives flexibility to the fabrication process (i.e., patterning and lamination may be performed in any order).

Moreover, a tensile test (engineering stress and strain test) was done on both the hot- and cold-laminated papers and compared with the results with the plain paper. These experiments were performed under two different conditions: when the laminated papers were wet and when they were dry. Figure 3d shows the stress–strain curve, yield strain and stress, and ultimate strain and stress of these five different samples. The results show that, by laminating the chromatography paper, we can improve the yield stress by around 3 fold with hot lamination and 1.5 fold with cold lamination. This improvment in strength is more critical after wetting, which simulated sample application: the wet chromatography paper could not tolerate the stress, but the laminated papers could bear a larger stress. Wetting the laminated papers reduces their yield stress by 25%–35%, but this strength was still greater than that of the nonlaminated wet paper.

Continuous Ink Supply. We have developed a continuous ink supply system (Figure 1c,d) to improve the cost-effectiveness and throughput of the fabrication. For this purpose, a commercially available hydrophobic solution has been dyed and used as the plotting agent. The ink was fed continuously into the technical pens (Figure 4a), which were

DOI: 10.1021/acs.analchem.7b01418
Anal. Chem. 2017, 89, 6351–6357

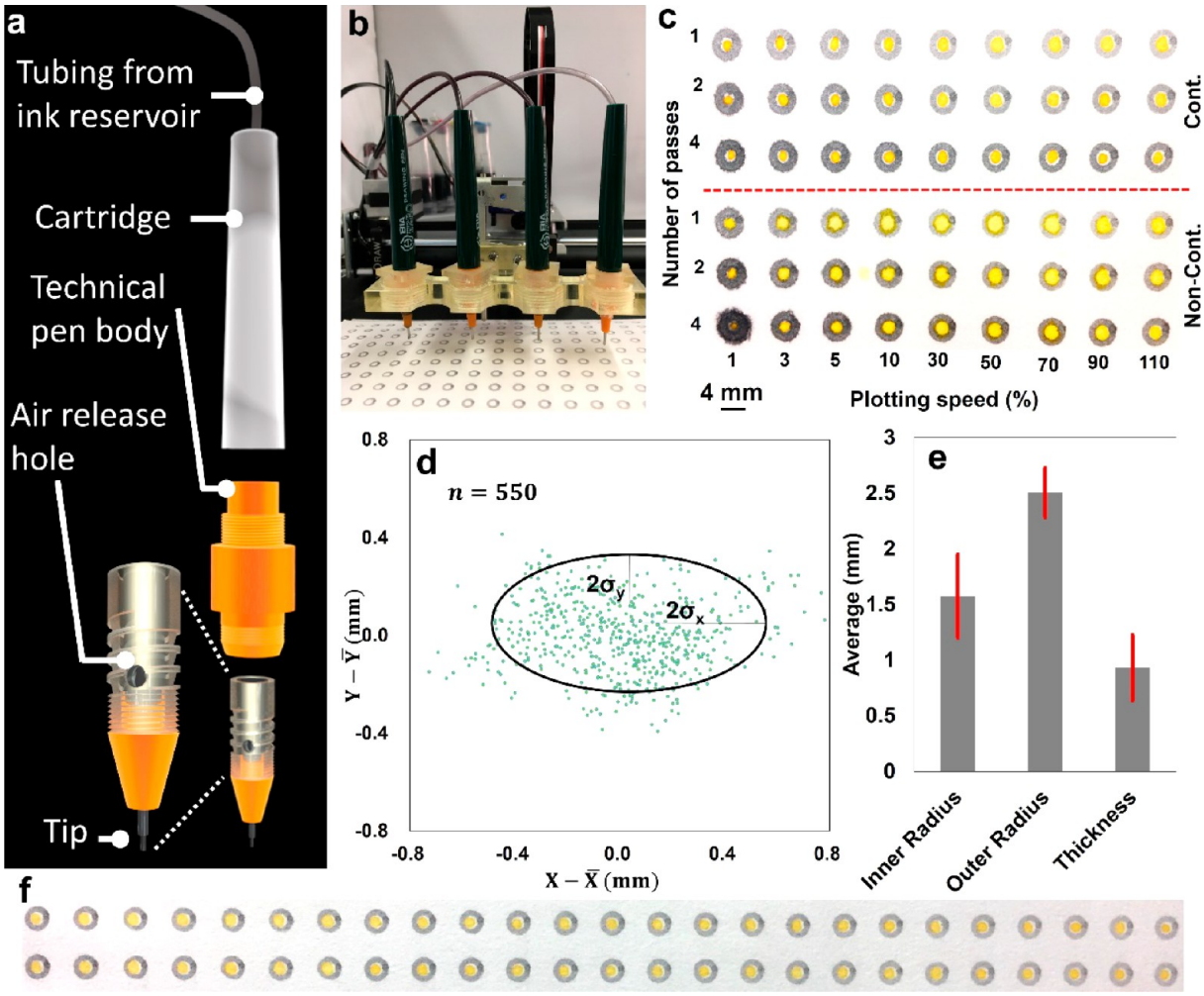

Figure 4. Performance of the continuous plotting system in high-throughput fabrication of paper-based microfluidics. (a) Illustration of continuous ink technical pen. We modified the technical pen by (i) sealing the air release hole of the technical pen and (ii) creating a hole at the top surface of the cartridge using a hand drill. (b) Technical pens fed continuously by ink. (c) Effect of different plotting speeds and number of passes on water resistance of patterns in continuous (top) and noncontinuous (bottom) plotting system. (d) Deflection of the plotted patterns in both the *X*- and *Y*-directions (n = 550). σ_x and σ_y are the overall standard deviations in the *X*- and Y-directions, respectively. $\bar{X}$ and $\bar{Y}$ are the mean deflections in the *X*- and *Y*-directions, respectively. (e) The mean and standard deviation of the inner and outer radii as well as the thickness of the plotted patterns with 50% plotting speed (n = 550). (f) A representative image shows the performance of the continuous plotting system in high-throughput fabrication of paper-based microfluidics.

contained in a multipen holder (Figure 4b). The setup was used to plot patterns in both the noncontinuous (using the internal cartridge of the technical pen) and continuous flow systems at different speeds. The water resistance of the prepared ink was investigated to confirm that the patterned hydrophobic barriers can effectively contain an aqueous sample in the hydrophilic testing region. The results in Figure 4c show that the prepared ink in both the noncontinuous and continuous systems could block the flow of a dyed aqueous solution for plotting speeds ranging from 1 to 110%. Only a single pass was needed to effectively contain the sample in the testing region. During our tests, we did not experience any clogging at the tip of the technical pen; this can be partially attributed to the relatively high initial boiling point of the mineral spirit solvent (145−174°C) of the hydrophobic solution.

To evaluate the geometrical performance of the continuous-flow pen system, the deflection of the plotted circles was measured (Figure 4d). The accuracy was calculated from 550 plotted circles: the trueness was −0.2 mm in the *X*-direction and 0.1 mm in the *Y*-direction, and the precision (95% confidence ellipse) was 0.5 mm in the *X*-direction and 0.3 mm in the *Y*-direction. These values are similar to those obtained with the permanent marker system. The coefficient of variation for the inner and outer radii (i.e., the roundness of the plotted circles) were 29% and 9%, respectively, which is similar to that obtained using the marker. Further, the coefficient of variation in the line thickness of the plotted patterns (Figure 4e) was 32%, which indicates greater consistency than with the marker.

To demonstrate the throughput of the proposed continuous system, we plotted 550 circles with 4 mm diameter at 50% plotting speed with a single pass. To test the water resistance of the circles, the dyed aqueous solution was used (Figure 4f shows a representative group of circles). The results show that about 95% (523 out of 550) of the circles were able to contain the aqueous sample within the testing region. The total time needed to plot 550 circles was about 12 min using only a single pen; this time can be further reduced by implementing the multipen holder (Figure 4b).

DOI: 10.1021/acs.analchem.7b01418
Anal. Chem. 2017, 89, 6351−6357

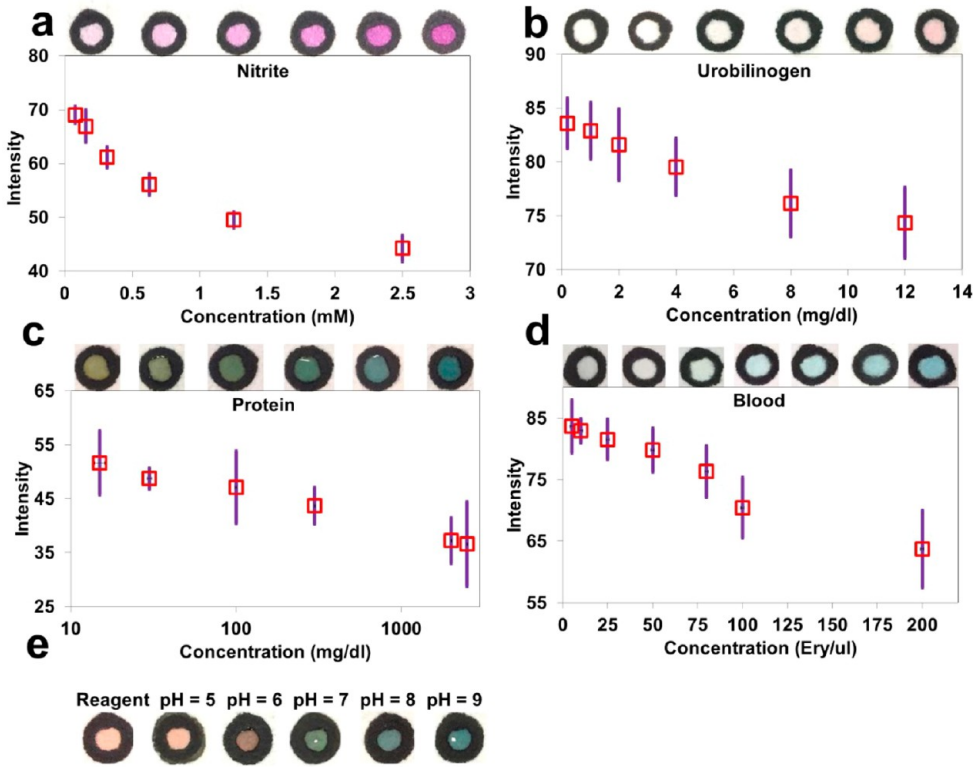

Figure 5. Colorimetric chemical assays. The quantified results of the effect of (a) nitrite, (b) urobilinogen, (c) protein (bovine serum albumin), and (d) blood concentrations on color intensities. (e) Effect of pH of solution on color intensity.

Colorimetric Biological Assays. To verify the applicability of our fabrication method, we conducted colorimetric biological assays which are useful for clinical urine analysis: nitrite, urobilinogen, protein, blood, and pH assays (Table S-2).[28−30] We measured the color formation of various colorimetric reagent solutions as a function of the analyte concentration (for blood, different numbers of cells per milliliter were used) (Figure 5a−d). The color intensity increased as the analyte concentration increased in each assay, as previously reported.[22−24] To investigate the ability to measure pH, we used buffers with different pH values ranging from 5 to 9 (Figure 5e). The observed color change was consistent with that which was previously reported.[22−24] The results show that the hydrophobic barriers were sufficient to contain the colorimetric reagents and the sample during the reaction so that the color change can be observed.

CONCLUSION

Considering the need for a cost-effective, high-throughput fabrication method for paper-based microanalytical diagnostic devices, we proposed a method using a pen plotter and hydrophobic marker. In this method, the pen plotter deposits a hydrophobic solution onto a hydrophilic paper to delineate the reaction area where the reagents are contained and the sample is applied. To increase the throughput and decrease the time and cost for fabrication of paper-based microfluidics, we used a custom-designed, low-cost multipen holder to enable multiplexing of the patterning process with up to eight printing heads. We simultaneously utilized multiple markers and decreased the fabrication time dramatically. Another improvement for the throughput of the fabrication method was developing a continuous ink supply system. We demonstrated patterning of 550 circular regions in ∼12 min (and can be further reduced to ∼3 min using multiple pens) with an estimated cost of less than $1. Testing the water resistance of 550 circular regions shows 95% fabrication success.

Furthermore, to increase the durability, stability, and mechanical strength of the fabricated microfluidic devices, we laminated the papers with hot- and cold-laminating layers. Using laminated papers in the fabrication of paper-based microfluidic devices was shown to not only improve their mechanical properties but also make handling the devices much simpler. To demonstrate the potential biochemical analytical capabilities of the fabrication method, we conducted five colorimetric biological assays: nitrite, urobilinogen, protein, blood, and pH. The novel method proposed here offers low cost, rapid, and simple fabrication of high-resolution paper-based microfluidic devices, which can be useful for mass production of paper-based microfluidics in both resource-limited and developed countries.

ASSOCIATED CONTENT

Supporting Information

The Supporting Information is available free of charge on the ACS Publications website at DOI: 10.1021/acs.analchem.7b01418.

Materials, design and 3D printing of the multipen holder, lamination of the paper, continuous ink supply, colorimetric biological assays, accuracy of patterns drawn by using eight pens simultaneously vs a single pen (Figure S-1), pattern used for calculating the resolution of barriers and channels (Figure S-2), and means and standard deviations of deflections (Table S-3) (PDF)

DOI: 10.1021/acs.analchem.7b01418
Anal. Chem. 2017, 89, 6351−6357

AUTHOR INFORMATION

Corresponding Author

*E-mail: savas.tasoglu@uconn.edu.

ORCID

Savas Tasoglu: 0000-0003-4604-217X

Author Contributions

×R.A. and F.G. contributed equally to this work

Notes

The authors declare the following competing financial interest(s): S. Tasoglu and S. Knowlton are founders of and have equity interest in mBiotics, LLC, a company that is developing microfluidic technologies for point-of-care diagnostic solutions. The interests of S. Tasoglus and S. Knowlton were viewed and managed in accordance with the conflict of interest policies. The authors have no other relevant affiliations or financial involvement with any organization or entity with a financial interest in or financial conflict with the subject matter or materials discussed in the manuscript apart from those disclosed.

ACKNOWLEDGMENTS

S.T. acknowledges the American Heart Association Scientist Development Grant (Grant 15SDG25080056) and the University of Connecticut Research Excellence Program award for financial support of this research. S.K. acknowledges the support of the National Science Foundation Graduate Research Fellowship (DGE-1247393).

REFERENCES

(1) Anciaux, S. K.; Geiger, M.; Bowser, M. T. *Anal. Chem.* **2016**, *88*, 7675−7682.

(2) Bruno, G.; Canavese, G.; Liu, X.; Filgueira, C. S.; Sacco, A.; Demarchi, D.; Ferrari, M.; Grattoni, A. *Nanoscale* **2016**, *8*, 18718−18725.

(3) Liang, Y.-R.; Zhu, L.-N.; Gao, J.; Zhao, H.-X.; Zhu, Y.; Ye, S.; Fang, Q. *ACS Appl. Mater. Interfaces* **2017**, *9*, 11837−11845.

(4) Macdonald, N. P.; Cabot, J. M.; Smejkal, P.; Guijt, R. M.; Paull, B.; Breadmore, M. C. *Anal. Chem.* **2017**, *89*, 3858−3866.

(5) Amin, R.; Knowlton, S.; Hart, A.; Yenilmez, B.; Ghaderinezhad, F.; Katebifar, S.; Messina, M.; Khademhosseini, A.; Savas, T. *Biofabrication* **2016**, *8*, 022001.

(6) Sivashankar, S.; Agambayev, S.; Alamoudi, K.; Buttner, U.; Khashab, N.; Salama, K. N. *Micro Nano Lett.* **2016**, *11*, 654−659.

(7) Songjaroen, T.; Dungchai, W.; Chailapakul, O.; Henry, C. S.; Laiwattanapaisal, W. *Lab Chip* **2012**, *12*, 3392−3398.

(8) Tian, L.; Morrissey, J. J.; Kattumenu, R.; Gandra, N.; Kharasch, E. D.; Singamaneni, S. *Anal. Chem.* **2012**, *84*, 9928−9934.

(9) Mentele, M. M.; Cunningham, J.; Koehler, K.; Volckens, J.; Henry, C. S. *Anal. Chem.* **2012**, *84*, 4474−4480.

(10) Sameenoi, Y.; Panymeesamer, P.; Supalakorn, N.; Koehler, K.; Chailapakul, O.; Henry, C. S.; Volckens, J. *Environ. Sci. Technol.* **2013**, *47*, 932−940.

(11) Jokerst, J. C.; Adkins, J. A.; Bisha, B.; Mentele, M. M.; Goodridge, L. D.; Henry, C. S. *Anal. Chem.* **2012**, *84*, 2900−2907.

(12) He, Q.; Ma, C.; Hu, X.; Chen, H. *Anal. Chem.* **2013**, *85*, 1327−1331.

(13) Hossain, S. Z.; Luckham, R. E.; McFadden, M. J.; Brennan, J. D. *Anal. Chem.* **2009**, *81*, 9055−9064.

(14) Cai, L.; Wu, Y.; Xu, C.; Chen, Z. *J. Chem. Educ.* **2013**, *90*, 232−234.

(15) Whitesides, G. M. *Nature* **2006**, *442*, 368−373.

(16) Sechi, D.; Greer, B.; Johnson, J.; Hashemi, N. *Anal. Chem.* **2013**, *85*, 10733−10737.

(17) de Tarso Garcia, P.; Cardoso, T. M. G.; Garcia, C. D.; Carrilho, E.; Coltro, W. K. T. *RSC Adv.* **2014**, *4*, 37637−37644.

(18) Yetisen, A. K.; Akram, M. S.; Lowe, C. R. *Lab Chip* **2013**, *13*, 2210−2251.

(19) Li, X.; Tian, J.; Shen, W. *Anal. Bioanal. Chem.* **2010**, *396*, 495−501.

(20) Olkkonen, J.; Lehtinen, K.; Erho, T. *Anal. Chem.* **2010**, *82*, 10246−10250.

(21) Carrilho, E.; Martinez, A. W.; Whitesides, G. M. *Anal. Chem.* **2009**, *81*, 7091−7095.

(22) Xia, Y.; Si, J.; Li, Z. *Biosens. Bioelectron.* **2016**, *77*, 774−789.

(23) He, Y.; Wu, Y.; Fu, J.-Z.; Wu, W.-B. *RSC Adv.* **2015**, *5*, 78109−78127.

(24) Li, X.; Tian, J.; Garnier, G.; Shen, W. *Colloids Surf., B* **2010**, *76*, 564−570.

(25) Peeling, R.; McNerney, R. *Increasing Access to Diagnostics through Technology Transfer and Local Production*, WHO: Geneva, Switzerland, 2011.

(26) Nie, J.; Zhang, Y.; Lin, L.; Zhou, C.; Li, S.; Zhang, L.; Li, J. *Anal. Chem.* **2012**, *84*, 6331−6335.

(27) Pollock, N. R.; Rolland, J. P.; Kumar, S.; Beattie, P. D.; Jain, S.; Noubary, F.; Wong, V. L.; Pohlmann, R. A.; Ryan, U. S.; Whitesides, G. M. *Sci. Transl. Med.* **2012**, *4*, 152ra129−152ra129.

(28) Klasner, S. A.; Price, A. K.; Hoeman, K. W.; Wilson, R. S.; Bell, K. J.; Culbertson, C. T. *Anal. Bioanal. Chem.* **2010**, *397*, 1821−1829.

(29) Martinez, A. W.; Phillips, S. T.; Butte, M. J.; Whitesides, G. M. *Angew. Chem., Int. Ed.* **2007**, *46*, 1318−1320.

(30) Lin, S.-C.; Hsu, M.-Y.; Kuan, C.-M.; Wang, H.-K.; Chang, C.-L.; Tseng, F.-G.; Cheng, C.-M. *Sci. Rep.* **2015**, *4*, 6976.

DOI: 10.1021/acs.analchem.7b01418
Anal. Chem. 2017, 89, 6351−6357